Supplementary Information (SI) for Sensors & Diagnostics.
This journal is © The Royal Society of Chemistry 2025

Electronic Supplementary Information (ESI)

CO_2-sensitive inks for the rapid measurement of total viable count (TVC) using micro-respirometry

Sean Cross, Christopher O'Rourke and Andrew Mills*

School of Chemistry and Chemical Engineering, Queens University Belfast, Stranmillis Road, Belfast, BT9 5AG, UK

S1 Predicted bacterial growth and %O_2 depletion

A continuous logistic equation is often used to describe bacterial growth kinetics, based on the assumption that the rate of growth, d$N(t)$/dt, at any time t, is proportional to the size of the population, $N(t)$, and the remaining material resources in the growth medium. The integrated form of the rate equation is,

$$N(t) = N_{max}/[1 + A^*\exp(-kt)] \qquad \text{(S1)}$$

where N_{max} is the maximum number of bacteria the growth medium can support, A* = (N_{max}/N_o - 1), k is a proportionality constant, and N_o is the initial bacteria population at t = 0. In μR-TVC, the observed variation of %O_2 with time, starting with an air-saturated solution with %O_2 = 21%, produces a %O_2 vs t profile which is the mirror image of the $N(t)$ vs t bacterial growth curve described by eqn (S1). This profile can be described by the following expression,

$$\%O_2 = 21(1 - 1/[1 + A^*\exp(-t^*)]) \qquad \text{(S2)}$$

where t^* = -kt and is a unitless time parameter. Plots of the variation in $N(t)$ and %O_2 vs t^*, calculated using eqns (1) and (2), are illustrated in Fig. S1 below, assuming N_{max} and N_o are 10^8 and 10^4 CFU/mL, respectively.

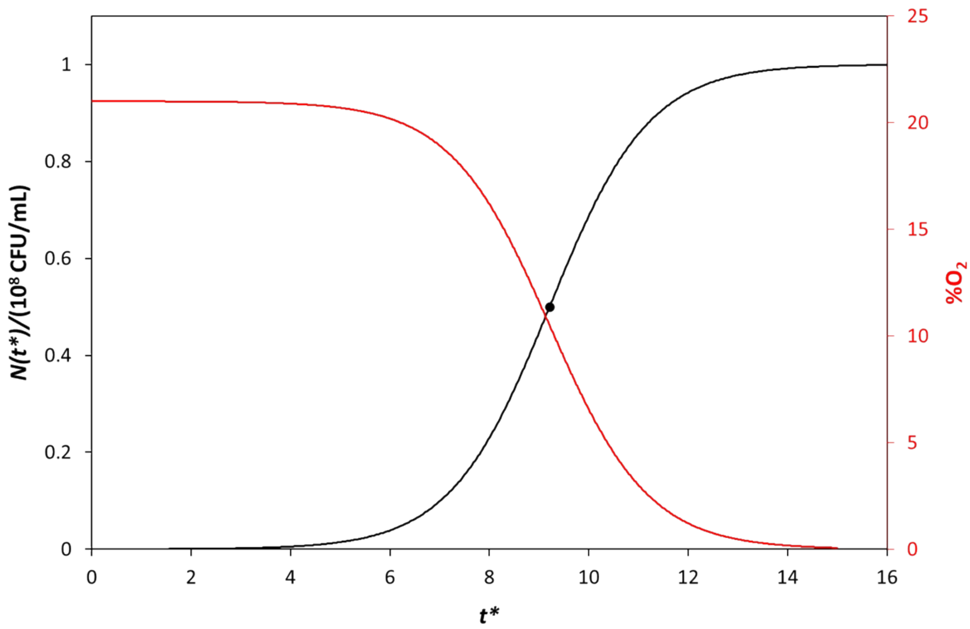

Fig. S1 Plots of the variation in $N(t^*)$ and %O_2 vs t^*, calculated using eqns (S1) and (S2), respectively, assuming N_{max} and N_o are 10^8 and 10^4 CFU/mL, respectively. The black point marks the t^* value ($t^*_{1/2}$ = 9.2) when N_o/N_{max} = 0.5 and O_2 = 10.5%.

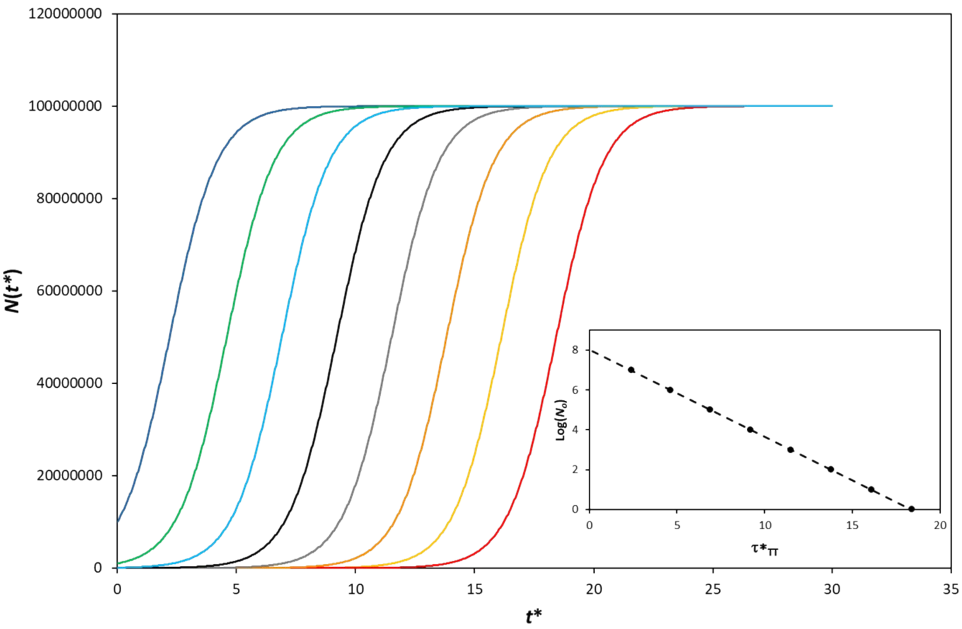

Fig. S2 Kinetic model, eqn (2), predicted plots of $N(t^*)$ (in 1 mL inoculant plus 9 mL growth medium incubated in a Falcon® tube) vs t* for N_o (in 1 mL inoculant) from 10^7 – 10^0 CFU/mL and subsequent plot of log(N_o) vs TT, where the value of TT was taken, from the data in the main diagram, as that of t^* when $N = 5x10^7$ CFU/mL.

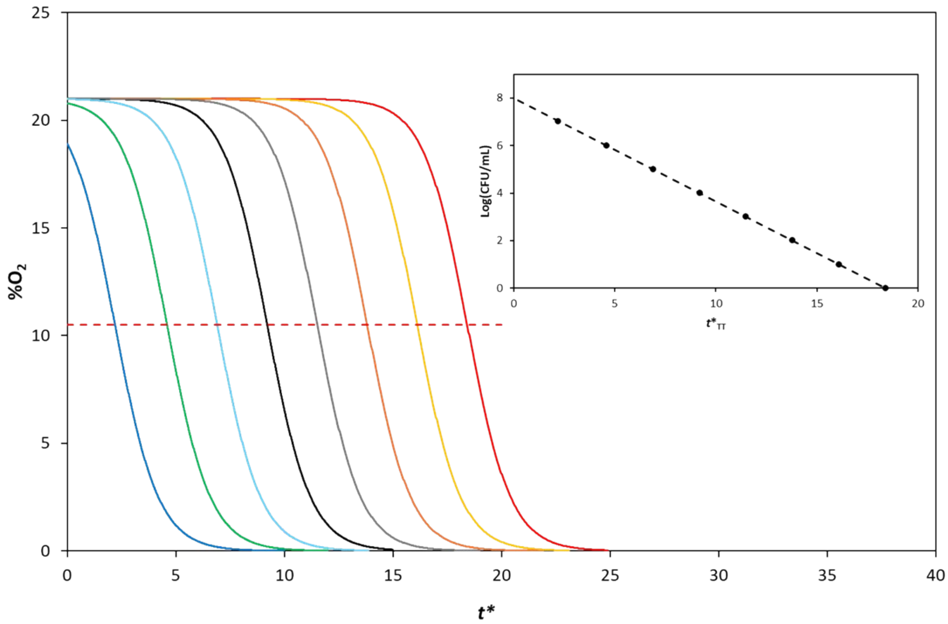

Fig. S3 Kinetic model, eqn (3), predicted plots of $\%O_2$ (under same reaction conditions as Fig. S2) vs t^* for N_o (in 1 mL inoculant) from (left to right) 10^7 – 10^0 CFU/mL and subsequent plot of log(N_o) vs TT, where the value of TT was taken, from the data in the main diagram, as that of t^* when $N = 5x10^7$ CFU/mL and $\%O_2 = 10.5\%$.

S2 Properties and structures of dyes used to make sensors and photographs of a typical heat-pressed CO_2 sensor.

Table S1. Properties and structures of the dyes used in heat-pressed CO_2 indicators.

Dye	pKa [1]	λ_{max} (DH) (nm)	λ_{max} (D^-) (nm)	Structure (DH)	Structure (D-)
CR	8.2	435	573	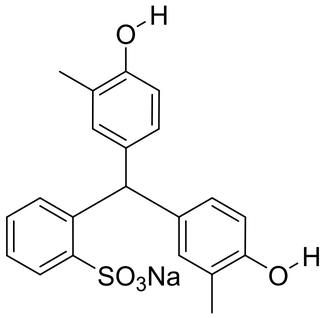	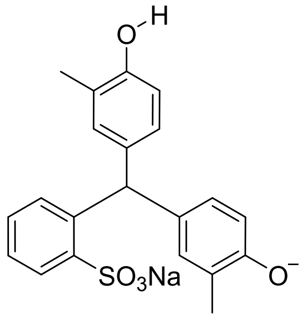
MCP	8.3	436	578	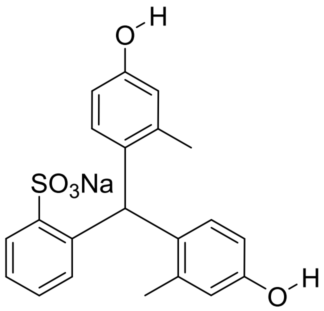	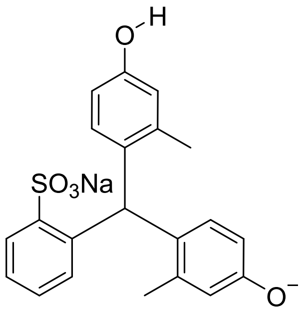
NP	8.5	652	N/A *	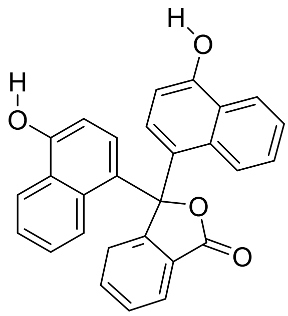	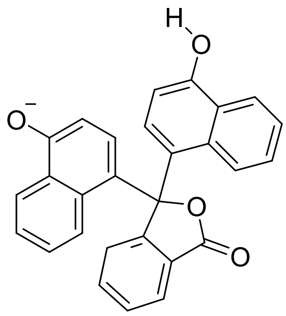
XB	8.9[2]	439	596	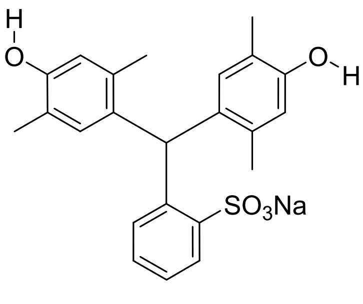	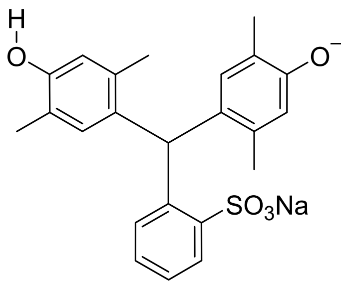

TB	8.9	436	595	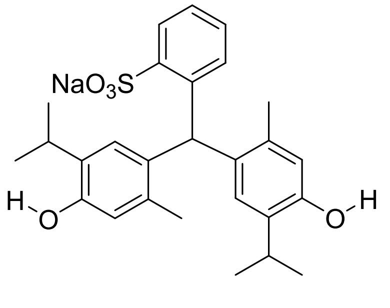	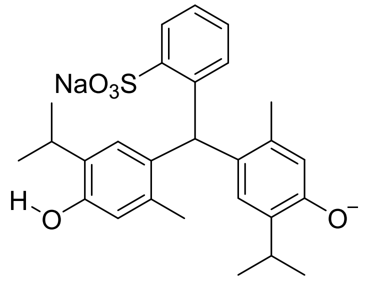
OCP	9.4	565	N/A*	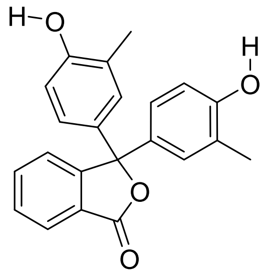	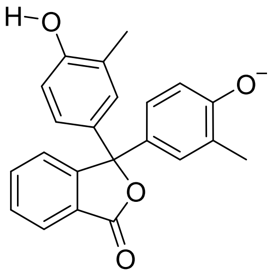
TP	10.0	595	N/A*	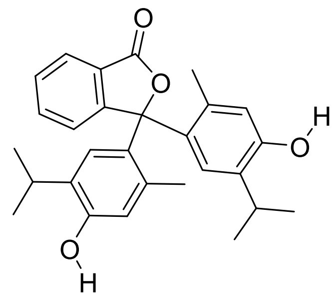	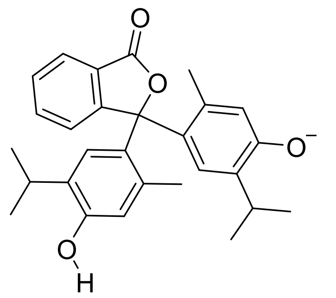

N/A*: Dye is colourless in its fully protonated (DH) form.

CR: cresol red, MCP: *m*-cresol purple, NP: α-naphtholphthalein, XB: xylenol blue, TB: thymol blue, OCP: *o*-cresolphthalein, TP: thymolphthalein.

1. R. S. Sabnis, in *Handbook of Acid-Base Indicators*, CRC Press, Boca Raton, FL, USA, 2008.
2. L. McDonnell, D. Yusufu, C. O'Rourke and A. Mills, *Sens. Actuators, B,* 2024, **412**, 135859.

S3 Typical CO_2 sensor appearance, stability and durability

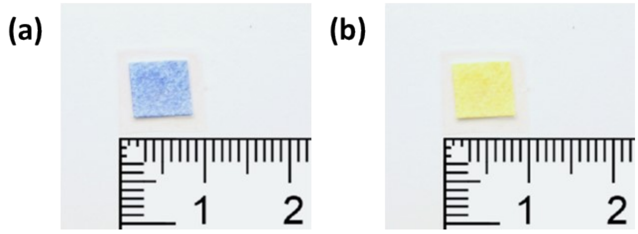

Fig. S4 Photograph of a typical, 1 cm square, heat-pressed XB-silicone sensor (5 mm square) in the (a) absence and (b) presence of 100% CO_2.

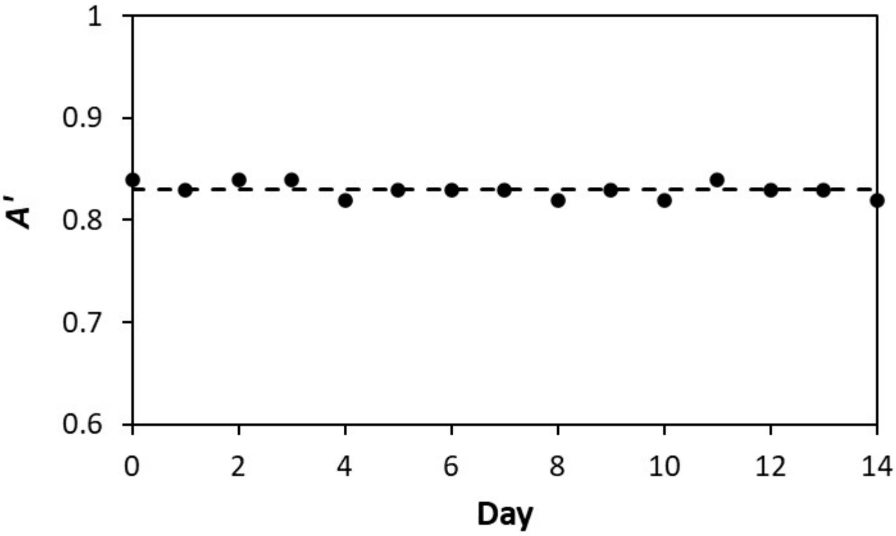

Fig. S5 Plot of the measured value of *A'* of a heat-pressed XB-silicone sensor placed in the LB growth medium at 30 °C and monitored over 14 days. The average measured value of $A' = 0.83 \pm 0.01$ (1.2%).

The results in Fig. S5 demonstrate the stability of the laminated CO_2 sensor in the growth medium used in all this work.

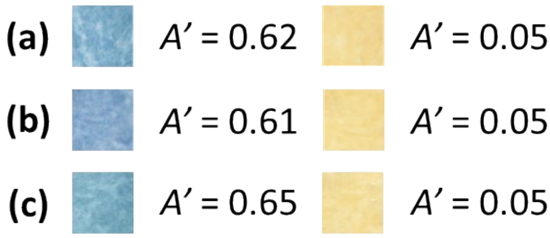

Fig. S6 Photographs of a heat-pressed XB-silicone indicator in a sealed glass vessel initially filled with (a) air (b) butane or (c) methane, before (blue) and after (yellow) injection of 1 mL of 100% CO_2.

The results in Fig. S6 demonstrate that a typical CO_2 sensor is unaffected by the presence of relatively inert gases, such as methane or butane. Lamination ensures that the sensor is also unaffected by non-gaseous ionic or neutral species present in the growth medium. Although the sensors are affected by other acidic, reducing and oxidising gases, such as SO_2 and NO_2, it is unlikely that these toxic gases would be produced in significant amounts in most TVC measurement studies.

S4 Sensor placement and use in a typical CO_2 μR-TVC run

Throughout this work, the CO_2-sensor under test was placed at the bottom of a 15 mL conical (Falcon®) tube, to which 9 mL of the sterile growth medium (LB broth) was added. The run was initiated by adding 1 mL of an *E. coli* dispersion of known bacterial load (e.g., 10^4 CFU/mL), after which the Falcon® tube was sealed and placed in an incubator set at 30 °C. The XB/silicone sensor was then photographed as a function of incubation time, *t*. A schematic illustration of a typical, inoculated and sealed Falcon® tube is shown in Fig. S7(a) in the ESI. Typically, multiple inoculations spanning a range of bacterial loads from 10^1 to 10^8 CFU/mL in tenfold steps were prepared in this manner, incubated simultaneously, and photographed at regular time intervals as a function of *t,* see Fig. S7(b) in the ESI. The incubation temperature was maintained at 30 °C in all cases.

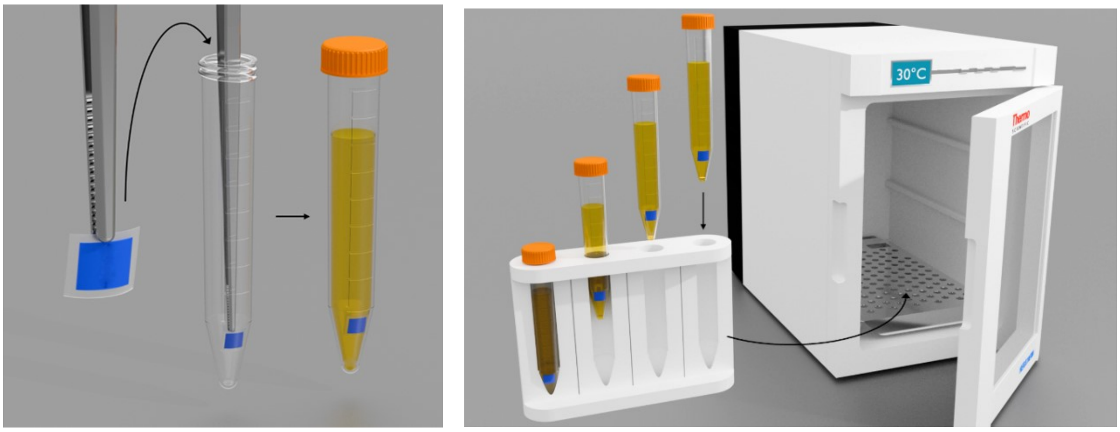

(a) **(b)**

Fig. S7 (a) Schematic illustration of a heat-pressed XB-silicone sensor placed in a Falcon® tube with 9 mL of growth medium and 1 mL of the bacterial inoculation and then sealed and (b) the tube in (a) placed in a rack, with other inoculated samples, which is then placed in an incubator at 30 °C with a clear window so that the all the colourimetric CO_2 sensors can be photographed as a function of incubation time, *t*.

S5 Reproducibility and accuracy of a typical CO_2 sensor

To evaluate sensor reproducibility, ten identical XB-LDPE solvent-based indicators were prepared and purged with gas mixtures containing different CO_2/air compositions (0% (argon), 0.1%, 1%, 5%, 25%, and 100%) at room temperature (20 °C) for 15 minutes, after which they were photographed. The resulting images, shown in Fig S8(a), were analysed using digital colour analysis (DCA), which yielded values of A'_o = 0.86 $\pm$ 0.04 and A'_∞ = 010 $\pm$ 0.003. For each sensor, the complete A' vs %CO_2 data set was used to construct a straight-line R vs %CO_2 plot using eqn (6), from which the sensitivity, α, was taken as the gradient. The average sensor sensitivity was found to be α = 0.74 $\pm$ 0.04 (5.4%) %CO_2^{-1}. The plot of A'_o, A'_∞ and α for the 10 sensors is illustrated in Fig. 8(b).

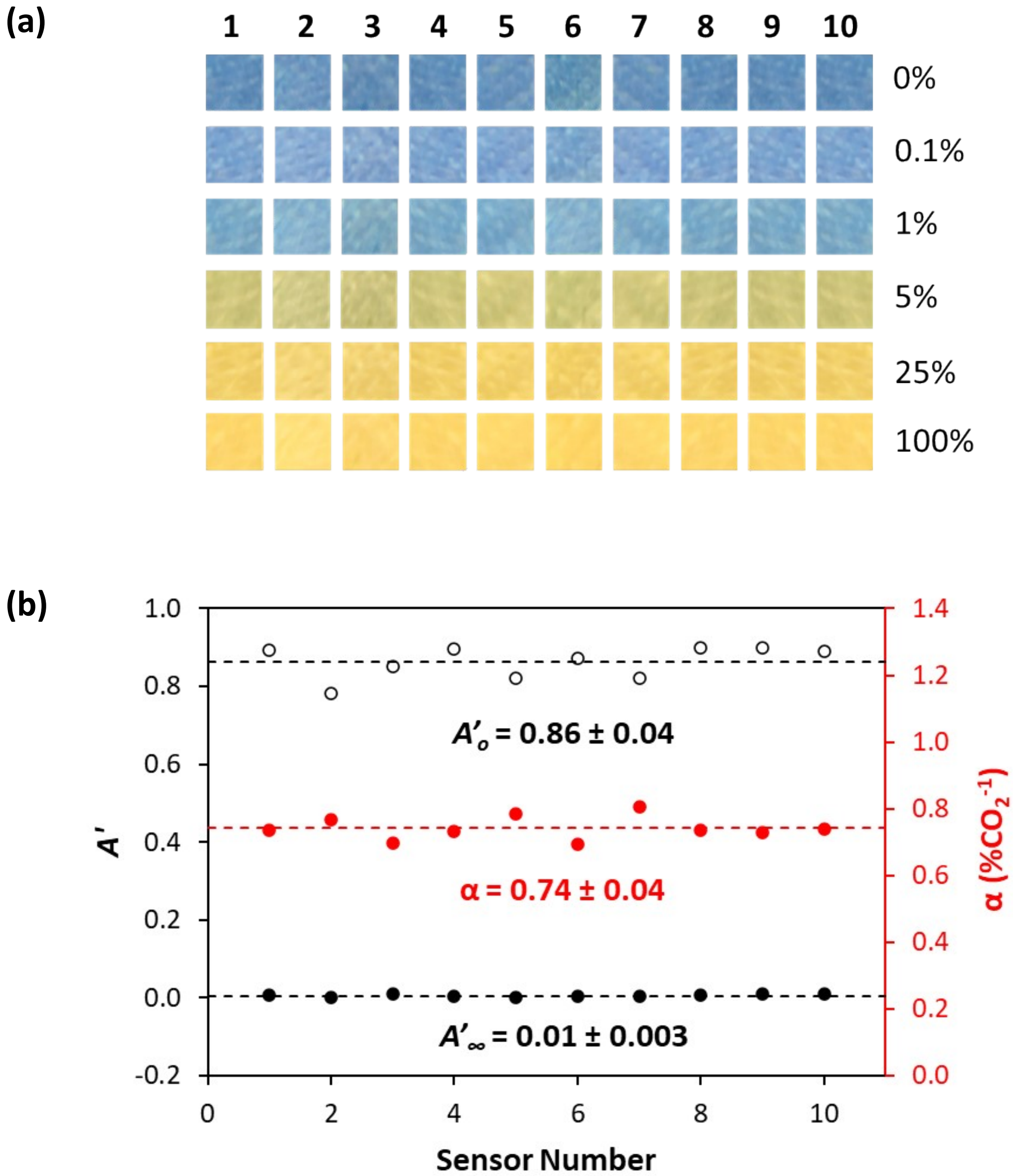

Fig. S8 (a) Photographs of 10 XB/silicone sensors exposed to different levels of CO_2 in air at 20 °C, (b) calculated A'_o, A'_∞ and α values for each of the 10 sensors determined using DCA analysis of the photographs in (a) and (for α) eqn (6).

S6 XB/silicone %CO_2 sensor response and recovery profile

The 90% response (0 to 5% CO_2), $t(90)_{\downarrow}$, and recovery (5 to 0% CO_2), $t(90)_{\uparrow}$, times of the XB/silicone CO_2 sensor at 20 °C were measured by monitoring A' as a function of time as it was exposed to a continuous cycle of air and 5% CO_2 sparging. The results of this work are illustrated in Fig. S9 below and revealed $t(90)_{\downarrow}$ and $t(90)_{\uparrow}$ values of 2.8 and 7.1 min, respectively.

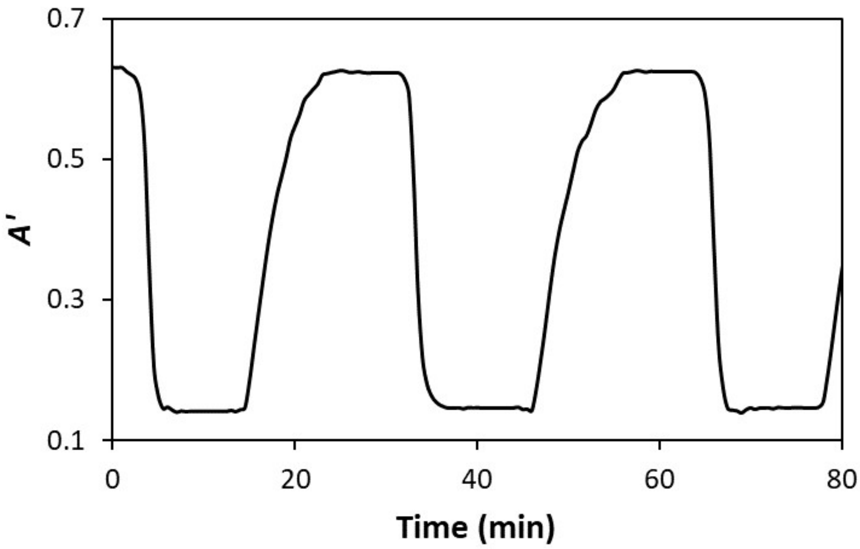

Fig. S9 Measured variation in A', derived from photographs of the sensor, as a function of time, t, for XB/silicone sensor at 20 °C upon exposure to a continuous cycle of air (high A') and 5% (low A') CO_2 sparging.

S7 Repeatability and durability of a typical CO_2 sensor in a CO_2 μR-TVC run

Ten identical XB/silicone sensors were prepared and individually placed into Falcon® tubes for a typical CO_2 μR-TVC run, using an *E. coli* inoculum of 10^4 CFU/mL. Each sensor was photographed as a function of incubation time, *t*, and the resulting photographs are illustrated in Fig. S10(a). DCA analysis of each set of photographs generated the ten plots of *A'* vs *t* illustrated in Fig. S10(b). From each plot, the halfway colour change point was identified, and the corresponding TT determined. A plot of the variation in TT for the 10 sensors is shown in Fig. S10(c) and demonstrates that a typical CO_2 sensor can be reproducibly made and used to generate consistent *A'* vs *t* profiles in CO_2 μR-TVC runs.

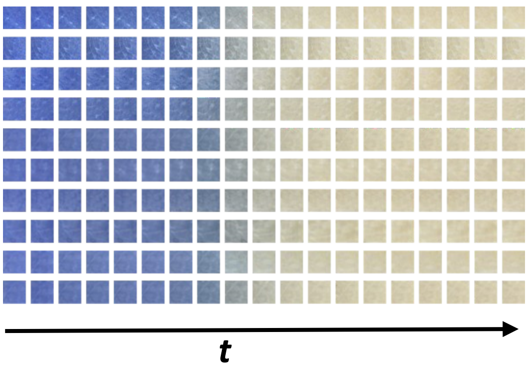

(a)

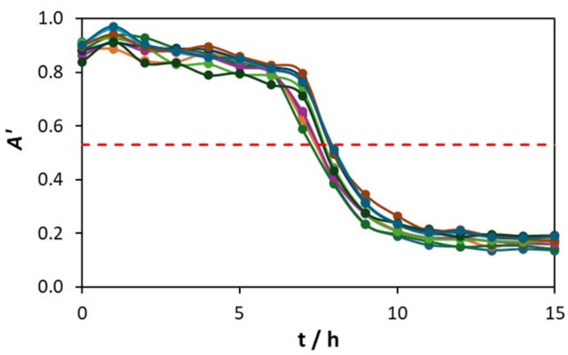

(b)

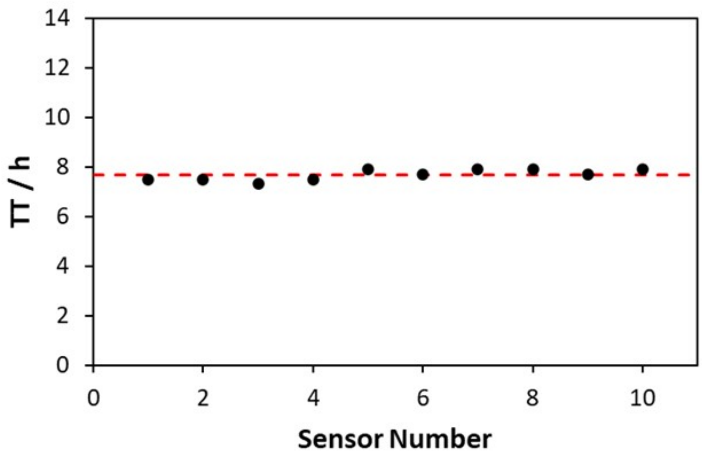

(c)

Fig. S10 (a) Photographs of ten XB/silicone sensors, each used in a typical CO_2 μR-TVC, as a function of run inoculation time, *t*, (b) ten *A'* vs *t* plots generated using DCA analysis of the photographs in (a) and (c) plot of TT vs sensor number, where each TT value was determined from the appropriate *A'* vs *t* in (b).

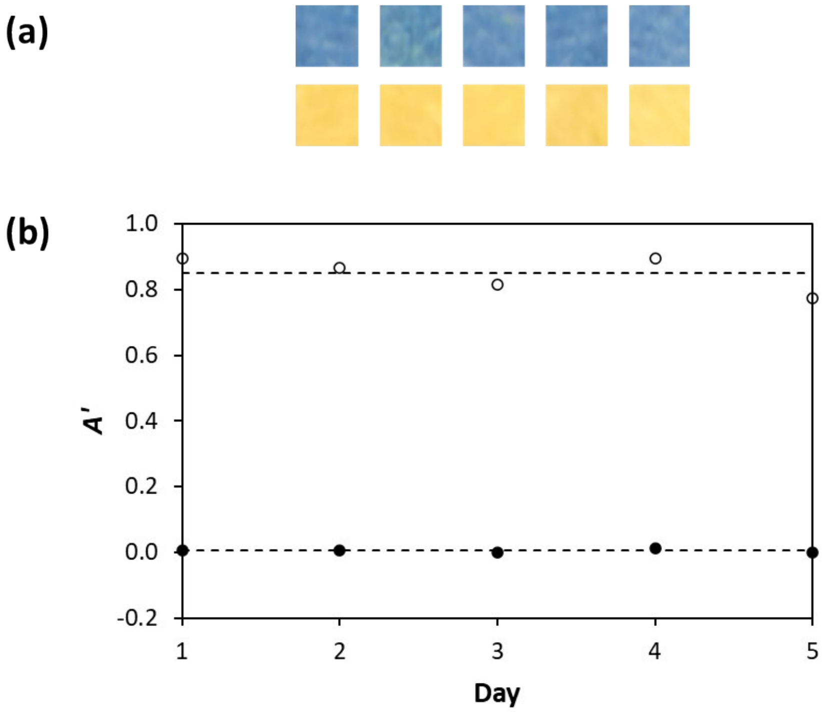

Fig. S11 (a) Plot of the measured values of A_o (in Ar) and A_∞ (in 100% CO_2) of the same XB/silicone sensor held in the same growth medium at 30 °C for 5 consecutive days. During this period the sensitivity of the sensor (α) remained unchanged at 0.74 %CO_2^{-1}.

The results in Fig. S11 demonstrate the durability of a typical CO_2 sensor, in that it can be used repeatedly over consecutive days and exhibit no sign of change in performance.

S8 The kinetic model and pH

For simplicity, the kinetic model in section 3 assumes that all CO_2 produced by the bacteria appears as dissolved CO_2 in the growth medium. In practice, this is unlikely, however the *shape* of the profile would be identical to that predicted by the model (see Fig. 2) if the pH of the growth medium remained constant during a run, as might be achieved using a pH buffer. For example, if the pH of the growth medium stayed at pH 7 through a kinetic run, only 18% of the total CO_2 generated would appear as dissolved CO_2. Thus, the real %CO_2 vs t curve would match the modelled shape but with all %CO_2 values scaled by a factor of 0.18. In this work, no additional pH buffer was added, and the pH was found to remain at pH 7 for 6 h before dropping to reach pH 6 after 10 h, as illustrated below in Fig. S12.

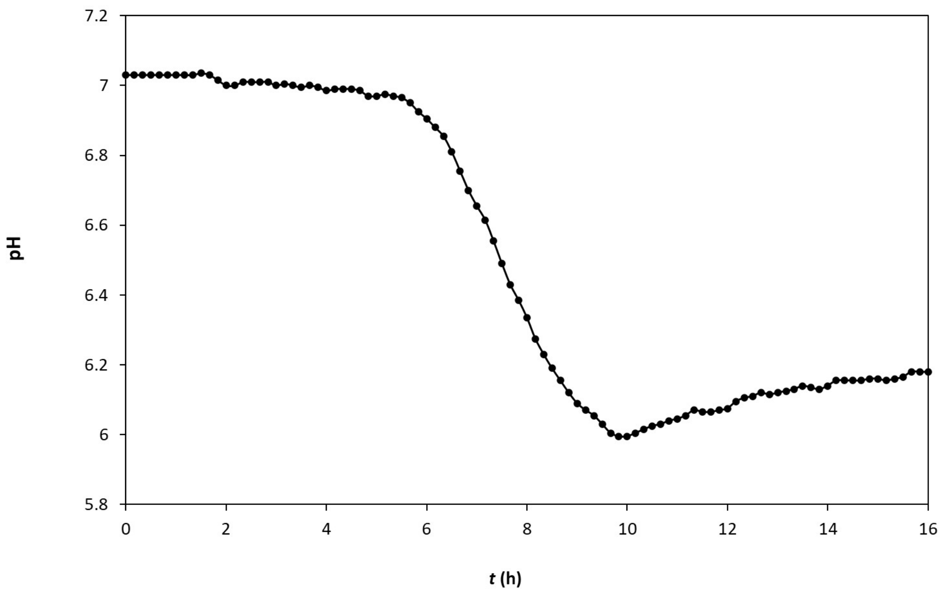

Fig. S12 Measured variation on pH in a typical kinetic run in which 10^4 CFU/mL of E. coli were used to inoculate 9 mL of the growth medium at 30^oC.

The effect of this pH change on the model-predicted %CO_2 and α vs t trends are illustrated in Fig. S13 and show that even with this change in pH the shapes of both curves are largely the same as those illustrated in Fig. 2. Thus, the key predicted feature of the model is maintained, that more sensitive CO_2 indicators yield lower TT values and thus faster analyses, as established experimentally by the TT vs α plot illustrated in Fig. 5.

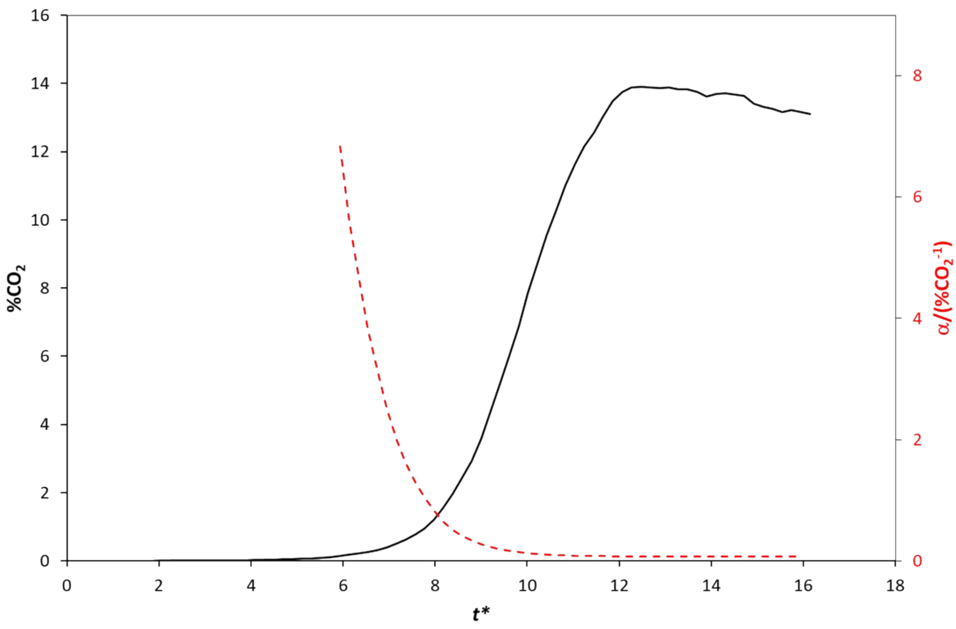

Fig. S13 Plot of the calculated variation in %CO_2 vs unitless time parameter *t**, assuming N_{max} and N_o are 10^8 and 10^4 CFU/mL, respectively. The broken red line is a plot of the calculated variation in t^*_{TT} for a series of CO_2 sensors with different sensitivity, α, values spanning the range 0.14 to 7 %CO_2^{-1}.

The calculated values of %CO_2 in Fig. S13 were derived for each value of *t** from the product of the %CO_2 values derived from eqn (7) and the fraction of CO_2 that would be detectable in the growth medium, $f(CO_2)$. The latter parameter is related to [H^+], and so the pH of the growth medium via the following expression,

$$f(CO_2) = [H^+]^2/([[H^+]^2 + [H^+]K_1 + K_1K_2) \quad \text{(S3)}$$

where K_1 and K_2 are the acid dissociation constants for bicarbonate and carbonate, respectively ($K_1 = 4.498\text{x}10^{-7}$ M and $K_2 = 4.79\text{x}10^{-11}$ M).[3]

To convert the real-time pH data (in h, from Fig. S12) into the unitless time parameter *t**, it was assumed that the mid-point in Fig. 2 (*t** = 9.2) corresponds to the mid-point in the pH profile (t = 7.0 h). Thus, all time points in Fig. S12 were converted to *t** values by multiplying by 9.2 / 7.0. The resulting $f(CO_2)$ vs *t** plot was then applied to the %CO_2 vs *t** data in Fig 2, calculated using eqn (7), to yield the adjusted %CO_2 vs *t** plot in Fig. S13.

3. W. G. Mook, in *Environmental isotopes in the hydrological cycle: principles and applications,* UNESCO, Paris, 2000, Chapter 9.